

Received August 11, 2018, accepted September 18, 2018, date of publication September 26, 2018, date of current version October 19, 2018.

Digital Object Identifier 10.1109/ACCESS.2018.2871725

Collision Avoidance of Podded Propulsion Unmanned Surface Vehicle With COLREGs Compliance and Its Modeling and Identification

XIAOJIE SUN¹, GUOFENG WANG, YUNSHENG FAN, DONGDONG MU, AND BINGBING QIU

School of Marine Electrical Engineering, Dalian Maritime University, Dalian 116026, China

Corresponding author: Guofeng Wang (gfwangsh@163.com)

This work was supported in part by the Nature Science Foundation of China under Grant 51609033, in part by the Nature Science Foundation of Liaoning Province of China under Grant 20180520005, and in part by the Fundamental Research Funds for the Central Universities under Grants 3132018306 and 3132016312.

ABSTRACT With the development of marine technology, the research of unmanned surface vehicles (USVs) has received wide attention from the world. Designing effective collision avoidance algorithm in dynamic sea environment is necessary for the navigation of USVs. This paper describes a collision avoidance system (CAS) with COLREGs compliance to improve autonomous navigational ability of USV. For small podded propulsion USV, a three-DOFs maneuvering model is established and the parameters of model are determined by the parameter identification method based on field experiments. About the COLREGs rules, the different maneuvering behaviors are summed up according to encounter situation and collision risk assessment. In the CAS, finite control set model predictive control is adopted, and COLREGs rules are taken as an evaluation standard in the quality function. Finally, the system is verified to avoid multiple dynamic obstacles and compliance vessel in the simulation and real environment, and the results of collision avoidance under four encounter situations are described in detail.

INDEX TERMS Unmanned surface vehicle, modeling, identification, collision avoidance system, finite control set, COLREGs.

I. INTRODUCTION

Unmanned surface vehicles (USVs) provide unique capabilities for military and security applications, including harbor patrol, maritime interdiction, and riverine operations [1]. All these capabilities require safe navigation in open waters, and the most important challenge is effective collision avoidance system (CAS) [2]. In recent years, more and more scholars have paid attention to the research of CAS, and have done some researches to solve this problem, for example, [3]–[6]. However, these studies only focus on avoiding collisions, but seldom consider compliance with the Convention on the International Regulations for Preventing Collisions at Sea (COLREGs) [7]. In the relevant reports [8] and [9], 56% of collisions at sea are related to the violation of the COLREGs rules. In order to use a reasonable collision avoidance operation and improve the USV autonomy, the COLREGs rules should be included in the design of the CAS, considering in three potential scenarios, such as overtaking, head-on, and crossing situation [1].

A. COLLISION AVOIDANCE AND COLREGs RULES

Some studies about collision avoidance of unmanned vessel have incorporated COLREGs rules into the CAS. Lee *et al.* [10] propose a heuristic search method based on Bandler to execute collision avoidance for autonomous ships, not only can derive a reasonable and safe path, but also comply with COLREGs. Kuwata *et al.* [11] and Bertaska *et al.* [12] introduce an autonomous motion planning algorithm based on velocity obstacles (VO) method to navigate safely and apply the rules simultaneously in dynamic environments. Inspired by Kuwata *et al.* [11], Zhao *et al.* [13] adopt the theory of evidential reasoning to assess risk, and the ORAC algorithm is applied to dynamic collision avoidance under the consideration of the rules. To avoid the compliance and non-compliance vessels, Zhang *et al.* [14] adopted a linear expansion algorithm, and collision avoidance operation includes the change of the course and speed. Campbell *et al.* [15] integrate obstacle detection, risk assessment and path planning into

an experimental platform, using heuristic path planning (R-RA*) algorithm to comply with COLREGs. Xu *et al.* [16] use the maneuver operational records conforming to the COLREGs from the European Ship Simulator in different encounter scenarios as samples, which is used to the predict collision avoidance operation by deep convolution neural network. However, [10], [13], [14], [16] of the above methods ignore static obstacles in design, or [11], [12], [15] are in a simple static and dynamic environment.

Based on the guidance, navigation, and control (GNC) system [2], after the guidance of the CAS, the controller of vessel needs to take corresponding actions, such as path tracking [6], [12]. But these control algorithms assume no obstacles in the process of control [1]. If the collision avoidance guidance algorithm is delayed or invalid, the vessel will lose the ability to avoid collision. Therefore, we need to combine collision avoidance and control into collision avoidance control algorithm, so that the control system also has the ability to avoid collisions. Johansen *et al.* [17] apply model predictive control (MPC) in the CAS of ship to solve this problem with a simple simulation environment. And in the field of ship motion control, MPC has been applied more widely. Li *et al.* [18] apply the MPC algorithm based on state-space equations to the ship dynamic positioning control system. Li and Sun [19] consider ship heading control with disturbance compensation based on the MPC. Some scholars mainly focus on the problem of ship tracking control based on MPC [20]–[22], but seldom consider it in ship collision avoidance. Compared with the ordinary ships, the USV is smaller and faster. So, the paper uses the finite control set model predictive control (FCS-MPC) algorithm with the fast dynamic response [23]. Since the algorithm has the ability of multi-objective optimization control, the COLREGs can be used as a constraint condition to optimize the control behavior, which makes the vessel avoid obstacles quickly on the premise of obeying the rules.

B. MODELING AND IDENTIFICATION

In terms of MPC, it is necessary to establish a mathematical model of vessel maneuvering motion [24]. The theoretical research on ship modeling has been developing for many years. In 1964, Abkowitz [25] proposed a small perturbation and Taylor expansion method to study the ship's plane motion model. Then, in 1970, a nonlinear ship motion mathematical model was developed by Norrbin [26], which avoids the lack of physical meaning in the model and forms a semi theoretical and semi empirical model. The two models mentioned above belong to the holistic model. Correspondingly, a separation motion mathematical model of ship was proposed by a research group called Maneuvering Modeling Group (MMG) in Japanese Towing Tank Conference (JTTC) and the outline was reported in the Bulletin of Society of Naval Architects of Japan in 1977 [27]. The MMG model is based on the hydrodynamics of the hull, propeller and rudder separately, and then studies the mutual interference between the parts of the propulsion and maneuvering system. Fossen [28], [29]

reviewed the surface vessel models in 1991 and published his monograph with a more detailed theoretical introduction in 2011. In the monograph [29], Fossen introduces the kinematics equation, rigid-body kinetics, hydrostatics, sea-keeping theory and maneuvering theory, and based on these theories, obtains the one degree of freedom (DOF) heading autopilot models and three-DOFs maneuvering models for surface vessel. But in contrast only a few articles study podded propulsion ship. In [30] and [31], the large ship with two pods propulsion was modeled. Mu establish the USV response model of podded propulsion to design the course controller [32]. For small podded propulsion USV, a three-DOFs maneuvering model is needed to design collision avoidance controller.

In order to obtain the specific model of the USV model, the parameters of model need to be determined by parameter identification method [33]. Model parameter identification is based on the known structure of the object model, by minimizing the error criterion function between the model and the object to determine the parameters of the model. A lot of research has been done on parameter identification of ship motion mathematical model. Cooper uses neural network to identify uncertain parameters or hydrodynamic coefficient in the model [34]. Some scholars also use the support vector machine (SVM) method to estimate the hydrodynamic coefficient [35] [36], or by the SVM with the artificial bee colony (ABC) [37] and the particle swarm optimization (PSO) [38]. In addition, some scholars have identified the four-DOFs ship model [39] and Abkowitz model [40] based on the least square algorithm. At the same time, gradient algorithm [41], genetic algorithm [41], [42] and kalman filter algorithm [43] have been widely used.

C. CONTRIBUTIONS

This paper is mainly aimed at solving the problem of collision avoidance about podded propulsion USV with COLREGs compliance. The main contributions can be summarized as follows:

- 1) By analyzing the force acting on the hull and the thrust force of pod, the three-DOFs maneuvering model of podded propulsion USV is derived.
- 2) On the basis of field experiments, the maneuvering model of USV is identified by the method of parameter identification method.
- 3) After analyzing the COLREGs rules, the collision risk is evaluated according to the Closest Point of Approach (CPA), and the three encounter situations are expanded to five, which are used to discuss the collision avoidance behavior that vessel should take under each situation.
- 4) Based on FCS-MPC method, a safe and fast CAS is proposed and has the ability to control USV collision avoidance and reach the target point.
- 5) The simulations are undertaken to avoid multiple dynamic cooperative obstacles (compliance vessels) and non-cooperative obstacles (non-compliance



FIGURE 1. The Lanxin USV.



FIGURE 2. The podded propulsion device of USV.

vessels and other obstacles) in the simulation and real environment, and the results of collision avoidance under four encounter situations are described in detail.

The remainder of the paper is organized as follows. Section II is an overview of the podded propulsion Lanxin USV and its system structure. Section III establishes the mathematical model of podded propulsion USV and identify the model parameters. After analyzing the COLREGs rules, Section IV summarizes different maneuvering behaviors according to meeting the conditions of collision risk assessment. In Section V, the CAS is designed based on FCS-MPC with COLREGs compliance. In Section VI, the CAS is verified to avoid multiple dynamic obstacles and compliance vessel in the simulation and real environment. Finally, some conclusions and future works are discussed in Section VII.

II. THE OVERVIEW OF LANXIN USV

A. LANXIN USV AND ITS POD

Lanxin USV is a small intelligence equipment platform of Dalian Maritime University, which has the function of maritime rescue, marine monitoring, water sampling and so on [32]. It is shown in Figure 1.

Figure 2 shows the podded propulsion device of USV. It can be seen that its propeller and rudder are integrated.

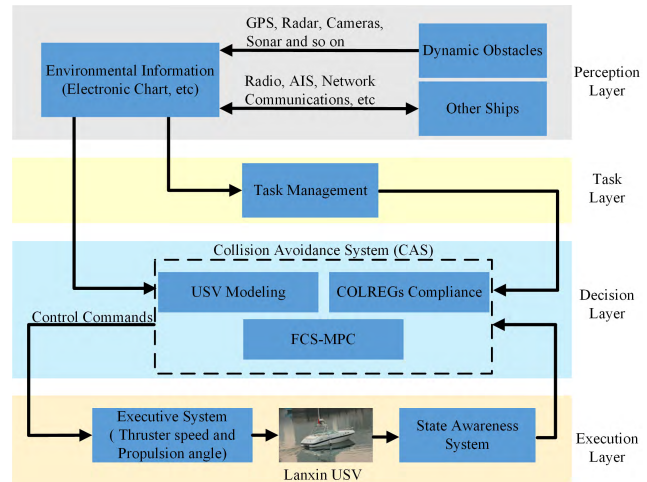


FIGURE 3. The hierarchical structure of USV system.

And the direction of vector thrust produced by the propeller is in accordance with the propulsion angle. Thus thruster and propulsion angle form its executive system.

B. THE HIERARCHICAL STRUCTURE OF USV SYSTEM

Figure 3 describes the hierarchical structure of USV system. It consists of four major layers, that is, Perception layer, Task layer, Decision layer and Execution layer. The USV needs to perceive external information using the Perception layer during its voyage. The global environment information can be obtained by electronic chart, and the surrounding environment by a range of different sensors such as Automatic Identification System (AIS), Global Positioning System (GPS), camera and marine radar. The Task layer can allocate the target point to the system according to the mission. Using the environment data obtained and target point, the CAS in the Decision layer determines the executive system command to safely navigate the USV. And in order to minimize system error, the real-time state information (velocity, position) is fed back to the Decision Layer to modify the control commands by state awareness system.

Of the four layers, the Decision layer plays the most important role in the USV system. The aim of CAS is to control the vessel from mission start and endpoints with collision avoidance and COLREGs compliance. It is important to avoid collisions in accordance with the rules. In sea environment, both static obstacles (islands and reefs) and dynamic obstacles (moving vessels) have potential collision risk for the USV. On the premise of compliance with rules, the CAS need to avoid these obstacles autonomously by maintaining safe distance. The CAS contains three components, i.e. USV modeling, COLREGs compliance and FCS-MPC. USV modeling and COLREGs compliance are the prerequisites and evaluation criteria of FCS-MPC. Their detailed description are given in Section III, IV and V. In addition, it is assumed that the state information of obstacles and USV can be detected exactly in real time.

III. USV MODELING AND IDENTIFICATION

A. KINEMATICS EQUATION OF USV

The kinematic equation of USV is used to describe the correspondence between the Earth-centered inertial (ECI) frame and body-fixed reference frame.

As shown in Figure 4, $O - X_0Y_0Z_0$ is the ECI frame and $o - xyz$ is the body-fixed reference frame. Here, δ is propulsion angle and (x, y) represents the position of the USV in the ECI frame. In actual navigation, the motion state of USV consists of six-DOFs including the surge velocity u , sway velocity v , heave velocity w , yaw rate r , rolling rate p and pitching rate q . However, according to the experience, too complex or too simple models are difficult to describe the movement characteristics of USV. In this article, only the horizontal movement of USV is considered, neglecting the roll, pitch and heave motions. The standard three-DOFs planar ship motion model is used as the model of USV [29], as shown in Figure 5.

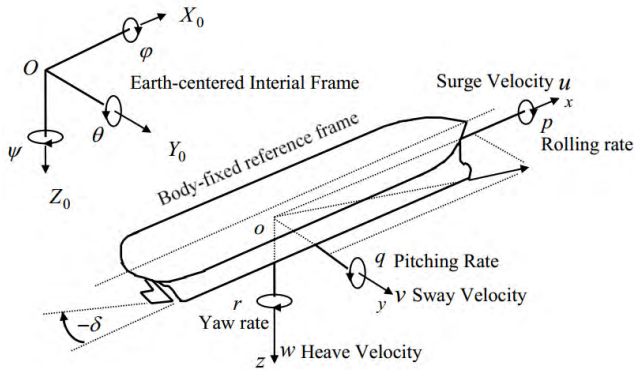


FIGURE 4. The Earth-centered inertial and body-fixed reference frame.

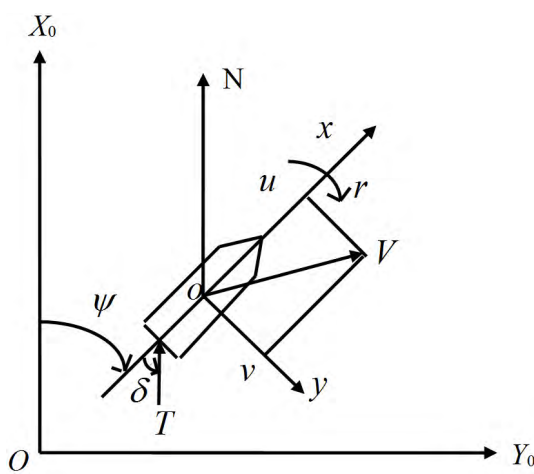


FIGURE 5. The standard three-DOFs planar ship motion variable description.

The kinematics equation transformation between the ECI frame and the body-fixed frame can be expressed as

$$\dot{\eta} = J(\psi)v \quad (1)$$

where ψ is the course angle, $\eta = [x, y, \psi]^T$, $v = [u, v, r]^T$, and $J(\psi)$ is rotation matrix.

$$J(\psi) = \begin{bmatrix} \cos(\psi) & -\sin(\psi) & 0 \\ \sin(\psi) & \cos(\psi) & 0 \\ 0 & 0 & 1 \end{bmatrix} \quad (2)$$

Then the kinematics equation of the system can be written as

$$\begin{cases} \dot{x} = u \cos \psi - v \sin \psi \\ \dot{y} = u \sin \psi + v \cos \psi \\ \dot{\psi} = r \end{cases} \quad (3)$$

The state quantity X of USV includes η and v , as

$$X = [x, y, \psi, u, v, r]^T \quad (4)$$

B. KINETIC EQUATION OF USV

Planar kinetic equation of three-DOFs is established by Lagrange mechanics theory [24].

$$M\dot{v} + C(v)v + D(v)v = \tau \quad (5)$$

where M is inertia matrix, $C(v)$ is Coriolis and centripetal matrix, $D(v)$ is Hydrodynamic Damping Matrix, $\tau = [\tau_u, \tau_v, \tau_r]^T$ represent the control forces and moment in all directions.

Assume that:

- 1) In the model the environmental interference can be ignored.
- 2) USV is symmetrical and the barycenter of USV coincides with the center of body-fixed frame. This is to say, the inertia, added mass and damping matrices are diagonal.

So, we can simplify the (5) to (6) [44], [45].

$$\begin{cases} \dot{u} = \frac{m_{22}}{m_{11}}vr - \frac{d_{11}}{m_{11}}u + \frac{1}{m_{11}}\tau_u \\ \dot{v} = -\frac{m_{11}}{m_{22}}ur - \frac{d_{22}}{m_{22}}v + \frac{1}{m_{22}}\tau_v \\ \dot{r} = \frac{m_{11} - m_{22}}{m_{33}}uv - \frac{d_{33}}{m_{33}}r + \frac{1}{m_{33}}\tau_r \end{cases} \quad (6)$$

Here, m_{ii} are given by the vessel inertia and the added mass effects, d_{ii} are given by the hydrodynamic damping.

For Lanxin USV, its actuator is a podded propulsion device, which is different from the ordinary propeller rudder separation propulsion device, resulting in a difference in the distribution of thrust. The force produced by the podded propulsion can be seen as a vector propulsion force T , as shown in Figure 5. The T is calculated in the way of [30] and [31]. So when the propulsion angle is δ , the vector thrust T in different directions is [32], [46]

$$\begin{cases} \tau_u = T \cos(\delta) \\ \tau_v = T \sin(\delta) \\ \tau_r = T \sin(\delta)L/2 \end{cases} \quad (7)$$

$$T = (1 - t_p) \rho n^2 D_p^4 K_T \quad (7)$$

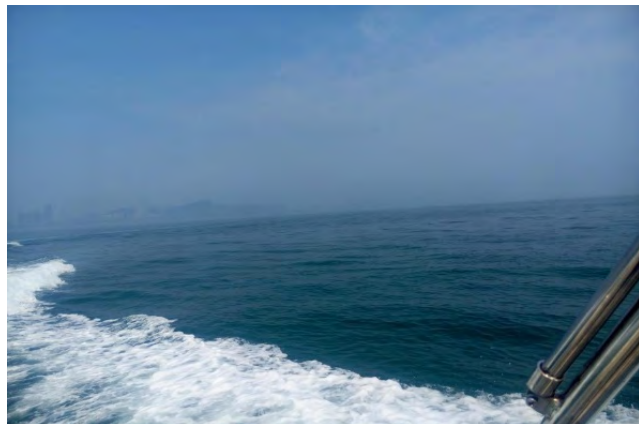


FIGURE 6. Experimental sea conditions.

where L is USV length, and the propulsion angle δ and thruster speed n are the inputs of model.

Based on the actual data collected from the experimental process about the steering process, the second-order link represents the steering gear response model [46], [47], that is

$$\ddot{\delta} + 2\zeta\omega_n\dot{\delta} + \omega_n^2\delta = K\omega_n^2\delta_r \quad (8)$$

here, δ_r is command propulsion angle, ω_n , ζ and K represent the natural frequency, damping ratio and proportionality coefficient, and the actual propulsion angle range is $|\delta| \leq 30^\circ$.

C. MODEL PARAMETER IDENTIFICATION

In order to identify the USV model, field experiments need to be done first. Field experiments include 10° turning test and $10^\circ/10^\circ$ zig-zag test. It is noteworthy that field experiments need to be carried out in a relatively stable sea surface. As shown in Figure 6, the sea surface is calm, and there is no obvious wave and current.

In the experimental process, the state X and input quantities δ , n are recorded in real time. Each equation in the kinematic model (6) of USV is a multiple-input single-output (MISO) subsystem, so the multiple-input multiple-output recursive least squares (MIMO-RLS) estimation method can be used to identify the three MISO subsystems.

In general, the MIMO-RLS needs to obtain the transfer function matrix model of the system, such as

$$G(z) = \frac{B(z^{-1})}{A(z^{-1})} = \frac{1}{A(z^{-1})} \begin{bmatrix} B_{11}(z^{-1}) & \dots & B_{1r}(z^{-1}) \\ \vdots & \ddots & \vdots \\ B_{m1}(z^{-1}) & \dots & B_{mr}(z^{-1}) \end{bmatrix} \quad (9)$$

where

$$\begin{cases} A(z^{-1}) = 1 + a(1)z^{-1} + a(2)z^{-2} + \dots + a(n_a)z^{-n_a} \\ B_{ij}(z^{-1}) = z^{-d_{ij}} [b_{ij}(0) + b_{ij}(1)z^{-1} + \dots + b_{ij}(n_{bij})z^{-n_{bij}}] \\ i = 1, 2, \dots, m; \quad j = 1, 2, \dots, r \end{cases}$$

Take third equations in the model (6), in which uv , τ_r are inputs, and r is the output. By discretizing the equation using Euler method with step h and Z transform, the conversion result is

$$r(k) = \frac{\left[\frac{m_{11}-m_{22}}{m_{33}}hz^{-1} \frac{1}{m_{33}}hz^{-1} \right] \cdot \begin{bmatrix} uv(k) \\ \tau_r(k) \end{bmatrix}}{1 + (\frac{d_{33}}{m_{33}}h - 1)z^{-1}} \quad (10)$$

That is

$$\begin{cases} A(z^{-1}) = 1 + \left(\frac{d_{33}}{m_{33}}h - 1 \right)z^{-1} \\ B(z^{-1}) = z^{-1} \left[\frac{m_{11}-m_{22}}{m_{33}}h \frac{1}{m_{33}}h \right] \end{cases}$$

Because the zig-zag test constantly changes the propulsion angle, it can better measure the maneuverability of ship than the turning test. Therefore, the identification data is from the $10^\circ/10^\circ$ zig-zag test, and the identification is further verified by the 10° turning test. The parameter identification through the data from $10^\circ/10^\circ$ zig-zag test, and the curves of identification are displayed in Figure 7.

Similarly, we can identify the other two equations, finally get the identification results: $m_{11} = 2652.25$, $d_{11} = 848.05$, $m_{22} = 2825.29$, $d_{22} = 10161.62$, $m_{33} = 4201.26$, $d_{33} = 22719.39$.

The steering gear response model is single-input single-output (SISO) system, which can be identified by ordinary RLS. The identification process also uses $10^\circ/10^\circ$ zig-zag test data, and the parameters of the steering gear response model is obtained by using the command propulsion angle δ_r as the input and the actual propulsion angle δ as the output. The parameters are $\omega_n = 2.84$, $\zeta = 1.53$, $K = 1.02$.

D. MODEL VALIDATION

1) ZIG-ZAG TEST VALIDATION

The USV and steering response model are used for $10^\circ/10^\circ$ zig-zag test simulation after the parameter identification. Under the condition of the same input quantities δ , n given as the actual data, the simulation is carried out and the Figure 8 shows the comparison between the simulation and actual results. Figure 8(a), 8(b) show the change of propulsion angles (command and actual propulsion angles) and heading angle respectively in simulation and field tests. In order to make a clearer comparison, the propulsion and the heading angles are compared in Figure 8(c). The steering cycles and heading angle of both are very close and the errors are less than 0.5s and 2° respectively except in the first period. Because the actual environment is complex, the errors are within the allowable range, which shows that the simulation model has high credibility.

Then, to further verify the model, the comparison of the state quantities u , v , r are shown in Figure 8(d). The data of u and r are in good agreement, but although the trend of v is the same, the error is relatively large, which is due to the interference of wind, wave and current to vessel sideslip in actual environment.

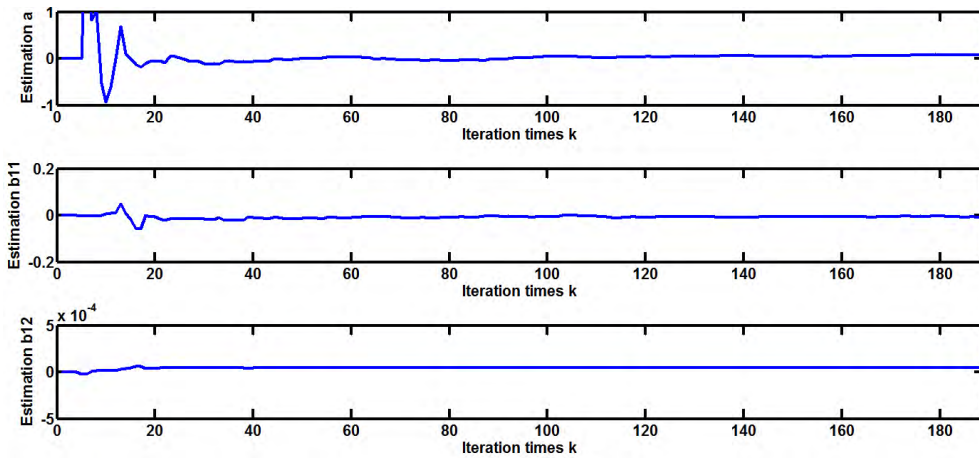


FIGURE 7. The identification curves.

TABLE 1. Results of evaluation index comprised of two environment.

Environment	Turning diameter	Surge velocity	Sway velocity	Yaw velocity
actual	79.94m	5.41m/s	-0.29m/s	8.62°/s
simulation	78.03m	5.48m/s	-0.28m/s	7.97°/s

2) TURNING TEST VALIDATION

Next, the accuracy and reliability of the model will be further verified from the turning test. Under the condition of the same input quantities given as the actual data, evaluations of the USV identification model in the simulation and actual environment are given in Table 1 and Figure 9. Table 1 describes the results of evaluation index in two environment. Figure 9 show the movement tracks and state quantities of the USV during the whole process.

The error between the simulation and actual results is also within the allowable range. This verification further proves the correctness of the identified model.

IV. COLREGs COMPLIANCE

The Convention on the International Regulations for Preventing Collisions at Sea (COLREGs) are designed by the International Maritime Organization (IMO) [10], requiring vessels to comply for preventing collisions between two or more vessels. Although the rules were made for vessels operated by the crew, the key elements could still be used as a reference for USV collision avoidance. In the COLREGs, there are 38 rules, which are divided into five parts, Part A (General), Part B (Steering and Sailing), Part C (Lights and Shapes), Part D (Sound and Light signals), and Part E (Exemptions). There are also four Annexes containing Positioning and technical details of lights and shapes, Additional signals for fishing vessels fishing in close proximity, Technical details of sound signal appliances and Distress signals. However, the main focus in this study is the Steering and Sailing rules, that is, the COLREGs Part B.

A. THE ENCOUNTER SITUATION

In order to avoid target vessels (TVs, other moving traffic vessels except for own vessel), it is necessary to determine the encounter situation and take corresponding measures according to the COLREGs. In COLREGs rule 13-15, the encounter situation is divided into Overtaking, Head-on and Crossing situation. But because the “crossing from left” and “crossing from right” require own vessel (OV) to perform distinctly different maneuvers in COLREGs, the study considers the following five situations: Overtaking (OT), Head-on (HO), Crossing from Left (LCS), and Crossing from Right (RCS), Safe encounter (SF). Each TV is categorized into a particular encounter situation based on its relative course (ψ_{TO}) and bearing with respect to the course of the OV (ψ_O).

First, according to the central circle in Figure 10, four regions are divided around the OV to distinguish the instantaneous position of the TV with respect to the course and position of the OV. The creation of the regions R1 to R4 is based on the requirements of COLREGs, and their boundary values are $\{67.5^\circ, 112.5^\circ, 202.5^\circ, 337.5^\circ\}$. Based on the Rule 13 of the COLREGs, which defines the OT situation, the boundary value of R3 is $\{202.5^\circ, 337.5^\circ\}$. But the Rule 14 about HO situation does not provide explicit division conditions except for the visibility of the masthead light and sidelights, which is defined to be small angles ($1 - 3^\circ$) in Annex I 9(a) of the COLREGs. However, the small angle makes the region R1 too narrow, and the encounter type is very sensitive for the change from HO to either RCS or LCS. In addition, considering Rule 14 (c) about HO, “when a vessel is in any doubt as to whether such a situation exists she shall assume that it does exist and act accordingly”, the enlarged R1 can avoid

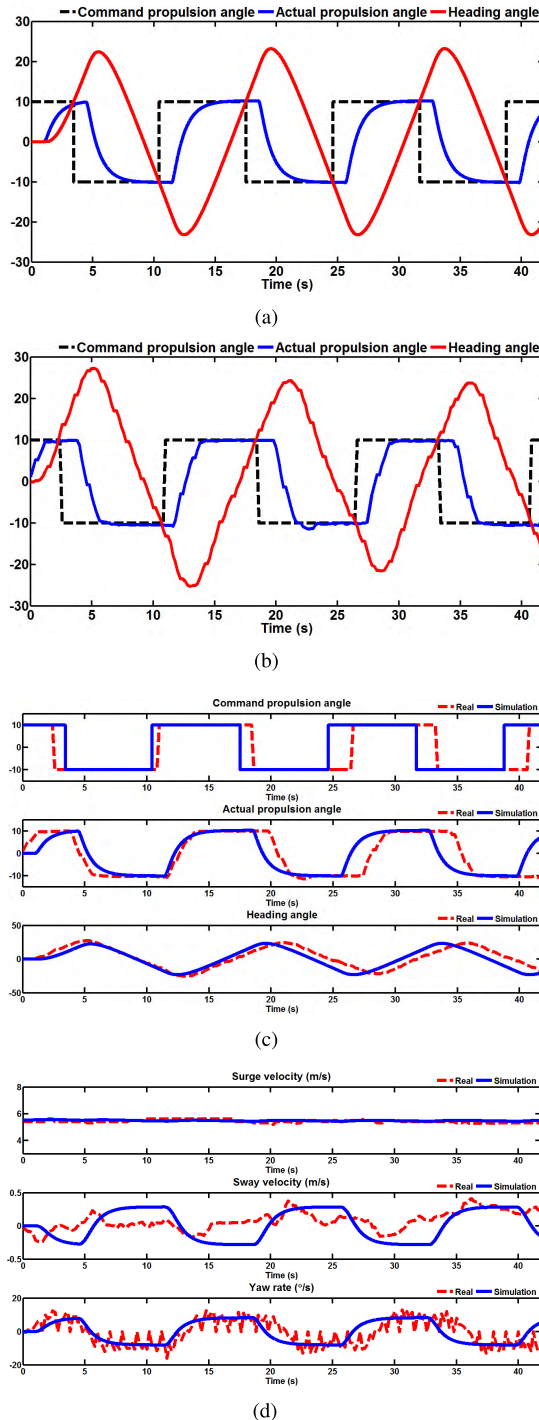


FIGURE 8. The comparison between the simulation and actual results in $10^\circ/10^\circ$ zig-zag test. (a) The propulsion and heading angles in simulation test; (b) The propulsion and heading angles in field test; (c) Comparison of the propulsion and heading angles; (d) Comparison of the state quantities.

the uncertainty of encounter situations. Therefore, according to the actual operation experience, the boundary value of R1 is determined as $\{67.5^\circ, 112.5^\circ\}$.

Next, based on relative course of TV with respect to the course of the OV, the TV is further divided by four small

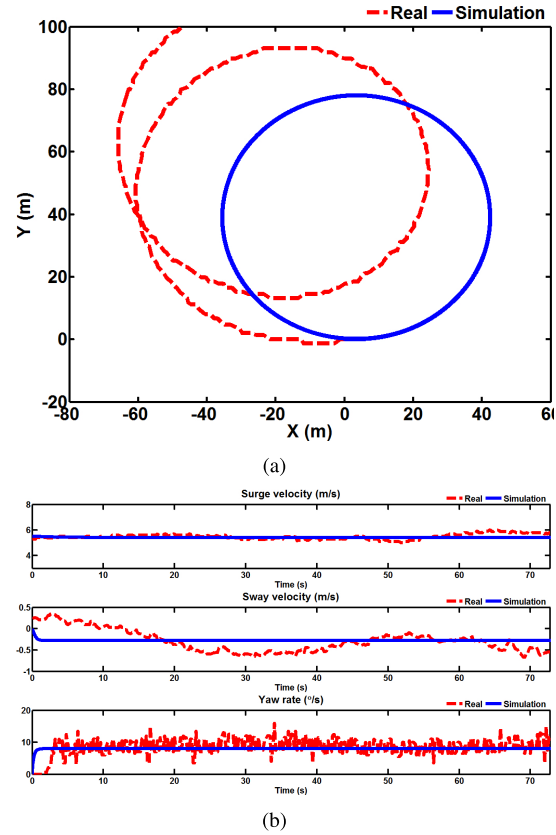


FIGURE 9. The comparison between the simulation and actual results in turning test. (a) the movement tracks; (b) the state quantities.

circles corresponding to the regions R1-4 in Figure 10, where encounter types are placed on each region of small circle. That is to say, when the TV is known from its bearing and course relative to the OV, the encounter type for the TV can be determined. Moreover, as stated in Rule 14 (c), the boundary between HO and Crossing encounters is HO encounters, where both vessels have to avoid collision.

After determining the encounter type, OV needs to take corresponding measures according to the COLREGs. In COLREGs rule 14 and 15, the HO and RCS situation require the vessel to alter its course to starboard. But there is no specific measures description about OT and LCS, so the OV shall make the corresponding measures according to the collision avoidance algorithm.

B. THE COLLISION RISK ASSESSMENT

It is also necessary to assess the extent of the collision when the vessels are encountered. This study adopts the calculation method of CPA (Closest Point of Approach), and assumes that the position and other parameters of vessels has been converted to Projection Coordinate System from Geographic Coordinate System, see Figure 11. The CPA contains two parameters called the time TCPA and distance DCPA to the closest point of approach between the OV and surrounding TVs. For a given time horizon, the closest distance when the

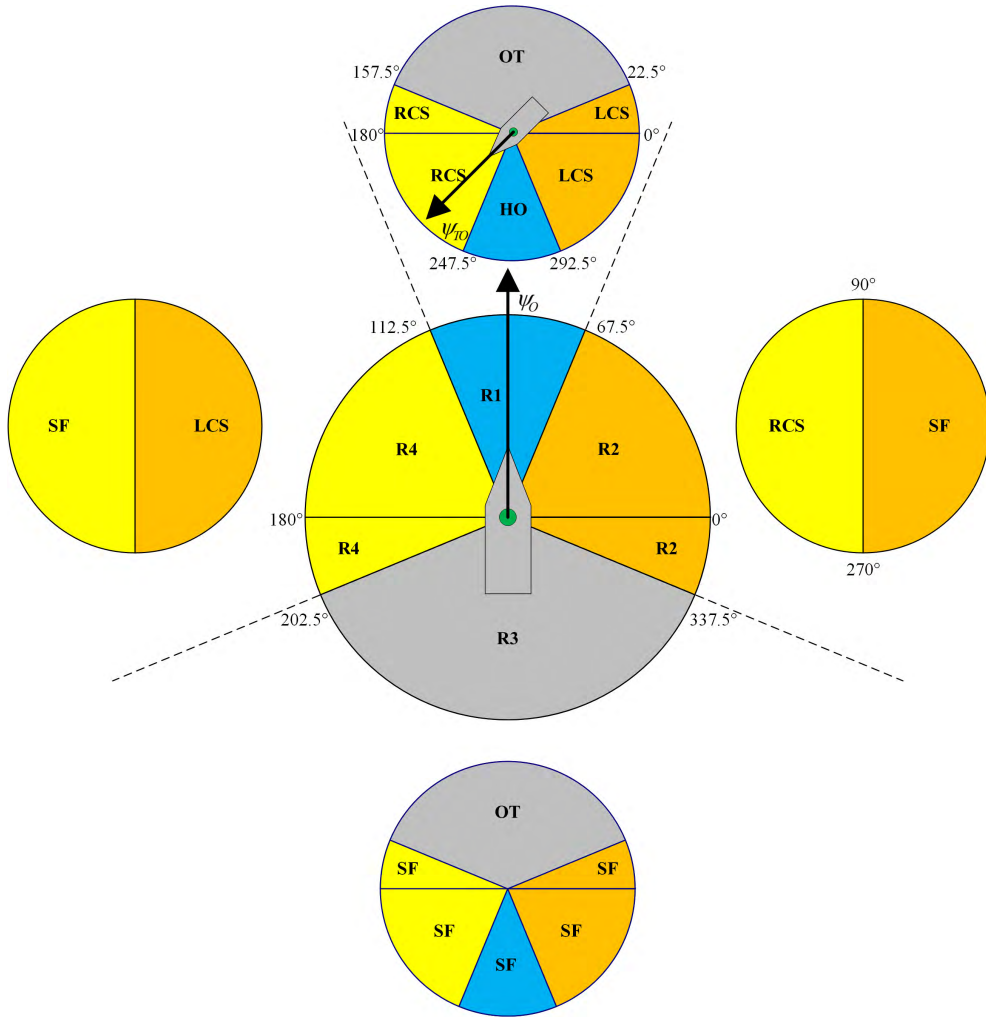


FIGURE 10. The division of encounter type.

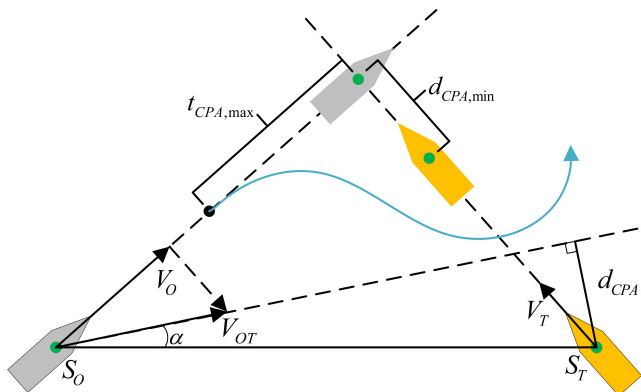


FIGURE 11. The collision risk assessment between own and target vessels by CPA method.

two vessels remain in their respective states is considered to be the CPA. The distance of two vessels to CPA is termed as the DCPA, the time to reach CPA is TCPA [48].

Given the position and velocity of OV and TV, the relative bearing and velocity of OV to TV are $S_{OT} = S_T - S_O$,

$V_{OT} = V_O - V_T$. α is the angle of V_{OT} to S_{OT} . The DCPA is given by [13]

$$d_{CPA} = \|S_{OT}\| \cdot \sin(\alpha) \quad (11)$$

The symbol of the DCPA is determined by the V_{OT} and S_{OT} . When TV passes the bow of the OV, the DCPA is positive; when the tail of the OV, the DCPA is negative.

The TCPA is then computed by [13]

$$t_{CPA} = \|S_{OT}\| \cdot \cos(\alpha) / \|V_{OT}\| \quad (12)$$

If the TV does not travel to CPA, the TCPA is positive; if has passed through CPA, the TCPA is negative.

For each TV, the CAS will examine whether there is a potential collision risk by checking if

$$\begin{cases} |d_{CPA}| < d_{CPA,\max} \\ 0 < t_{CPA} < t_{CPA,\min} \end{cases} \quad (13)$$

Here, the two conditions are described as: the computed DCPA is less than a user-defined maximum $d_{CPA,\max}$ and the user-defined TCPA is between zero and a user-defined

minimum $t_{CPA,\min}$. The $d_{CPA,\max}$ and $t_{CPA,\min}$ are generally determined by the user according to the size, speed, and turning radius of the USV.

In addition, COLREGS rules 8 and 16 require early action to avoid collisions. Therefore, the $d_{CPA,\max}$ and $t_{CPA,\min}$ should be set to larger values so that the course and speed have enough time to adjust.

V. COLLISION AVOIDANCE SYSTEM

A. THE AVOIDANCE CONTROL STRATEGY

The FCS-MPC divides the feasible control behavior into finite control sets, and the model of the system is used to predict the output variables of the model for each control set. By defining a selection criterion, the appropriate control set is selected and applied. The selection criterion can be expressed as a quality function, which is used to evaluate the predictive values of variables to be controlled by each possible control set. The selected control set makes the quality function optimal.

In the CAS of USV, the USV model is needed to predict the state quantity X . A block diagram of the proposed control strategy is shown in Figure 12. The avoidance control strategy is summarized in three steps:

- 1) The target point, environment model and state quantity $X(t_k)$ are obtained;
- 2) The USV model $f_p(X, S)$ is used to predict the state quantity $X_{pi}(t_{k+p})$ at time t_{k+p} for each control set $S_i(t_k)$, t_p is the prediction time.
- 3) Each control set $S_i(t_k)$ and their predicted state quantity $X_{pi}(t_{k+p})$ are evaluated by the quality function $f_Q(X_{pi}, S_i)$, and the control set S_o with optimize value for the quality function is applied to the vessel actuators.

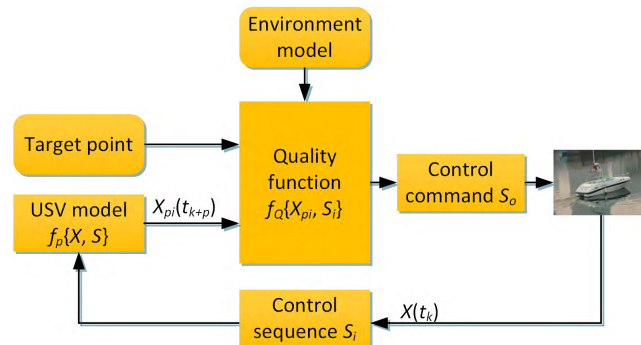


FIGURE 12. The block diagram of the control strategy in CAS.

B. FINITE CONTROL SET FOR USV

For the USV, there are two control actuators, namely propulsion angle δ and thruster speed n , and their actions are taken as finite sets. In this paper, regard to the fact that both change rate $\dot{\delta}$ and \dot{n} of two control actuators have to meet the hardware

limitation, in discrete time interval Δt the actuator actions is

$$S = \left\{ (\delta, n) \mid \begin{array}{l} \delta \in [\delta - \dot{\delta}\Delta t, \delta + \dot{\delta}\Delta t] \\ n \in [n - \dot{n}\Delta t, n + \dot{n}\Delta t] \end{array} \right\} \quad (14)$$

And their permissible ranges are expressed as follows

$$S_m = \{ \delta \in [-\delta_m, \delta_m], n \in [0, n_{\max}] \} \quad (15)$$

Considering the minimal discrete propulsion angle δ_d and thruster speed n_d , the amounts of control sets is

$$c = (2\dot{\delta}\Delta t/\delta_d) \times (2\dot{n}\Delta t/n_d) \quad (16)$$

When reducing the value of δ_d and n_d , the control behavior will be more detailed, but this will cause too much computation. So it is necessary to balance the number of control sets and the computational complexity.

C. THE QUALITY FUNCTION

According to the system requirements, the quality function $f_Q(X_{pi}, S_i)$ can be constructed using the predicted state quantity $X_{pi}(t_{k+j})$ and control set $S_i(k)$. The system requirements includes the five demands of the CAS, such as attainability, safety, compliance, stability and rapidity, so the function includes five corresponding subfunctions i.e. $f_1(X_{pi}, S_i)$, $f_2(X_{pi}, S_i)$, $f_3(X_{pi}, S_i)$, $f_4(X_{pi}, S_i)$, and $f_5(X_{pi}, S_i)$. And the control set S_o with maximize value for the quality function is selected. The five subfunctions are described as follows

1) ATTAINABILITY SUBFUNCTION $f_1(X_{pi}, S_i)$

Attainability can be guaranteed if the vessel course is always pointing to the target point, and the course is called the navigation angle. Therefore, the angle θ_{pi} between navigation angle and predicted course ψ_{pi} can evaluate attainability, as shown in Figure 13.

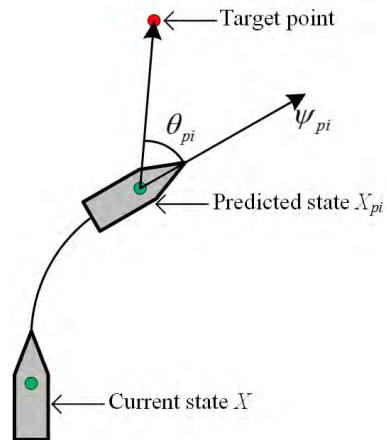


FIGURE 13. Description of attainability subfunctions.

The attainability subfunction is

$$f_1(X_{pi}, S_i) = \pi - \theta_{pi} \quad (17)$$

TABLE 2. Parameter information of the USV and CAS.

	Parameter	Value	Units
USV	Initial course of USV	90.0	°
	Initial speed of USV	0.0 (0.0)	m/s (kn)
	Initial thruster speed	0.0	r/min
	Maximum thruster speed	66.7 (4000)	r/s (r/min)
	Change rate of thruster speed	6.7	r/s ²
	Discrete thruster speed	1.7 (100)	r/s (r/min)
	Initial propulsion angle	0.0	°
	Maximum propulsion angle	30.0	°
	Change rate of propulsion angle	5.0	°/s
Algorithm	Discrete propulsion angle	1.0	°
	DCPA,max	300.0	m
	TCPA,min	30.0	s
	Detection area	500.0	m
	Distance range	200.0	m
	Prediction time	15.0	s
	Control update interval	1.0	s
Weight of evaluation function		(1.0, 2.0, 1.0, 0.5, 0.25)	—

2) SAFETY SUBFUNCTION $f_2(X_{pi}, S_i)$

The minimum distance do_i between vessel and z obstacles Xo can be used to describe safety in a distance range d_r . The safety subfunction $f_2(X_{pi}, S_i)$ is

$$f_2(X_{pi}, S_i) = do_i \quad (18)$$

among

$$do_i = \begin{cases} \min_{k=1}^z \{\bar{X}o_k\} & \text{if } \bar{X}o_k \leq d_r \\ d_{\max} & \text{else} \end{cases}$$

$$\bar{X}o_k = |Xo_k - X_{pi}|$$

where the Xo_k means the state quantity of the k th obstacle.

Moreover, in order to avoid potential collisions, stop distance d_{stop} also need to be considered. Based on the current speed V and acceleration \dot{V} of USV, it is calculated by

$$d_{stop}^i = V_{pi}^2 / (2 \cdot \dot{V}_{pi}) \quad (19)$$

And when $d_{stop}^i > do_i$, the i th control behavior S_i is eliminated.

3) COMPLIANCE SUBFUNCTION $f_3(X_{pi}, S_i)$

Compliance with the COLREGs enables the vessel to make the appropriate action. The collision risk assessment condition (13) and the division of encounter situation are given in Section IV. When the current situation satisfies the condition (13), the encounter situation is determined according to the bearing and relative course. As the only two encounter situation (RCS and HO) in COLREGs require the vessel to alter its course to starboard, it is necessary to adjust the propulsion angle to right. When the condition (13) is satisfied, the compliance subfunction is

$$f_3(X_{pi}, S_i) = \begin{cases} \delta_i - \delta & \text{if } \delta_i > \delta \& (\text{RCS or HO}) \\ 0 & \text{else} \end{cases} \quad (20)$$

4) STABILITY SUBFUNCTION $f_4(X_{pi}, S_i)$

The stability of vessel can be achieved by avoiding the large propulsion angle δ . So the stability subfunction is

$$f_4(X_{pi}, S_i) = \delta_m - |\delta_i| \quad (21)$$

5) RAPIDITY SUBFUNCTION $f_5(X_{pi}, S_i)$

The speed V of USV can express the rapidity as

$$f_5(X_{pi}, S_i) = V_{pi} \quad (22)$$

Then to smooth quality function the normalization method is used, for example, the normalized first subfunction is

$$\bar{f}_1(X_{pi}, S_i) = \frac{f_1(X_{pi}, S_i)}{\sum_{i=1}^c f_1(X_{pi}, S_i)} \quad (23)$$

Moreover, the five subfunctions can be taken care through adjusting the corresponding weighting factors $(\alpha, \beta, \gamma, \lambda, \zeta)$. The quality function is

$$f_{Qi}(X_{pi}, S_i) = \alpha \cdot \bar{f}_1(X_{pi}, S_i) + \beta \cdot \bar{f}_2(X_{pi}, S_i) + \gamma \cdot \bar{f}_3(X_{pi}, S_i) + \lambda \cdot \bar{f}_4(X_{pi}, S_i) + \zeta \cdot \bar{f}_5(X_{pi}, S_i) \quad (24)$$

Through the quality function, the system selects the optimal control command S_o , which can make the USV safe, compliant, stable and quick completion of the task.

VI. SIMULATIONS

In this section, simulations have been carried out in two different testing environments to validate the proposed CAS with COLREGs compliance. The purpose of the first test is to validate the ability of the algorithm to respectively avoid cooperative and non-cooperative obstacles with two different test scenarios in the simulation environment. The two test scenarios are designed as: 1) USV runs with three dynamic obstacles, and 2) Two USVs run together with four encounter situations. To further test the capability of the system dealing with actual collision avoidance, the second test runs in a real sea environment with model uncertainties and external disturbances, and describes the modeling of real environment. The moving cooperative and non-cooperative obstacles have been

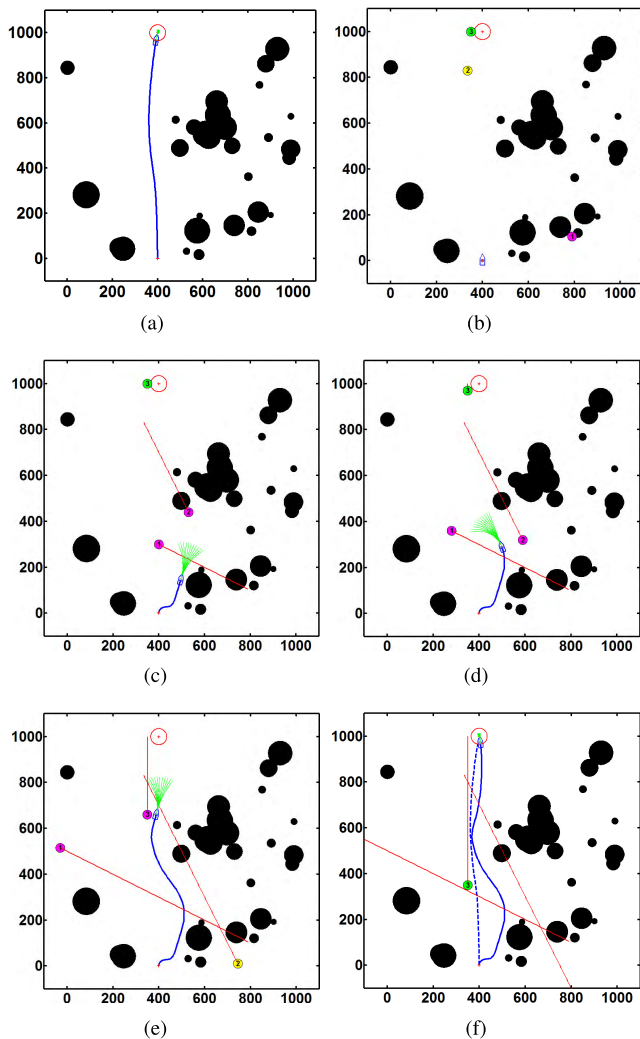


FIGURE 14. The motion sequence diagram of USV in static and dynamic simulation environment. (a) The final result in static environment; (b) The motion sequence diagram with time 1s in dynamic environment. (c) Time 40s. (d) Time 52s. (e) Time 83s.

added into the environment to construct a complex traffic situation. The parameters of the USV and CAS in Table 2 are applied to all tests. The CAS has been coded in Matlab, and simulated on the computer with a Core i7 3.6 GHz processor and 4 GB of RAM.

A. VERIFICATION IN SIMULATION ENVIRONMENT

In the first test, in order to simulate an area having enough space for USV to collision avoidance, the dimensions of area constructed are 1100 m × 1100 m. In Figure 14, the static obstacles are randomly generated 30 circular obstacles, the radius of which is from 10m to 60m. The start and end points are marked as red '+' and '*' markers, and the end point is enlarged to a red circular area. There are three curves in the figure. The blue and red curves represent the tracks of USV and dynamic obstacles (DO) up to a final time, respectively. The green curves are the current predicted trajectories. The cyan, yellow and green circles represent the

location of DO1, DO2 and DO3, and when they enters the detection area, the color of circle becomes magenta.

1) NON-COOPERATIVE OBSTACLES

First, USV runs in the static environment, and the final result is shown in Figure 14(a). USV safely avoids all obstacles to the end.

And then to test the capability of the CAS with COLREGs compliance to avoid dynamic obstacles, three DOs are added into the simulation environment at constant speed of 11m/s (DO1), 11m/s (DO2) and 10m/s (DO3) respectively, and three encounter situations, i.e. RCS, LCS and HO, are formed with USV. The simulated DOs can be seen as special mobile vessels without obeying the rules. Figure 14(b-f) are the movement sequences of the USV. Of this, Figure 14(b), 14(c) plot the USV alters its course to starboard in a RCS situation and avoid crossing ahead of DO1, which comply with Rule 15 of COLREGs. After avoiding the DO1, a LCS situation is made up of USV and DO2 in Figure 14(c). As DOs is not in compliance with these rules, Figure 14(d) display the USV takes action to avoid collision by maneuver of CAS with Rule 17(a) (ii). When successfully avoids the DO1 and DO2, the USV begins to form a HO situation with DO3 and starboard side turning is adopted by the CAS in Figure 14(e) (in compliance with Rule 14(a)). Figure 14(f) shows two tracks (blue solid curve and blue dashed curve) in dynamic and static environments.

Table 3 and Figure 15 show the results of algorithm performance evaluation in dynamic and static environments. Table 3 is the results of the evaluation index. Figure 15(a-d) describe the result of control behavior (thruster speed and command propulsion angle) and state output (speed and course of USV). It can be seen that USV can adjust speed and course according to collision risk and keep rapidity possible. In Figure 15(d), the larger command propulsion angle at the start stage is to comply with the rules and avoid obstacles. Figure 15(e) shows the computing time of CAS. And the update environment time is determined by the running time of the algorithm. As a result of the maximum running time 0.18s of CAS, the update environment time is set to 1.00s.

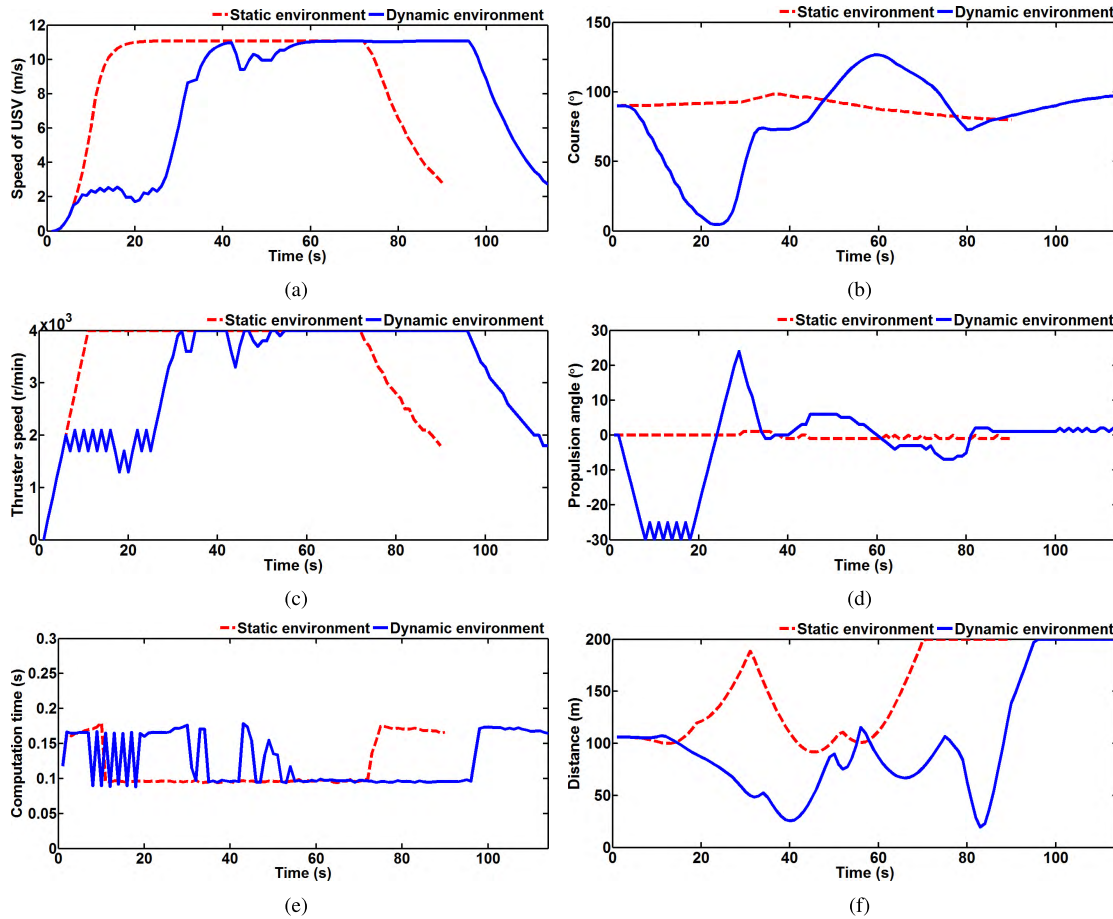
Safety is the most important measure for autonomous navigation and should be ensured during the whole process. Figure 15(f) represents the distance between the USV and the detected obstacles. In static environment, the minimum and average of the distance are 91.9m and 140.4m, and they are 19.5m and 101.4m in dynamic environment.

2) COOPERATIVE OBSTACLES

Next, the proposed method of CAS is tested with different encounter types between TV and OV, including Head-on (HO), Crossing from Left (LCS), Crossing from Right (RCS), and Overtaking (OT) in simulation environment. And to prove that COLREGs rules can be obeyed each other, the TV and OV are in compliance with the rules in whole process. In addition, the TV adopts the same CAS, USV model, and parameters as OV.

TABLE 3. Results of evaluation index comprised of two environment.

Environment	Index	Speed of USV(m/s)	Thruster speed(r/min)	Propulsion angle(°)	Computation time(s)	Distance(m)
static	maximum	11.0	4000	1.0	0.18	200.0
	minimum	0.0	0	-1.0	0.09	91.9
	average	9.0	3492	-0.4	0.25	140.4
dynamic	maximum	11.1	4000	24.0	0.18	200.0
	minimum	0.0	0	-30.0	0.09	19.5
	average	7.7	3183	-2.6	0.13	101.4

**FIGURE 15.** Evaluation results. (a) Speed of USV; (b) Course of USV; (c) Thruster speed; (d) Command propulsion angle; (e) Computation time; (f) Distance between obstacles and USV.*a: HEAD-ON SITUATION*

The first test scenario is a HO encounter with TV coming head-on towards OV. The test is to assess whether CAS is complying with COLREGs Rule 14, so that each vessels shall pass on the port side of the other. By testing in a relatively sparse area, the initial course of the opposite direction will generate a HO situation, and the rule be observed on the basis of the maneuver behavior and trajectories of the two vessels. Figure 16 shows a motion simulation and evaluation results of both vessels performing a starboard maneuver in order to pass on the port side of the other. And the symbols of OV and TV are blue and red boat forms. In the figure, both vessels are maneuvering according to COLREGs Rule 14 and pass each

other port to port. This test also verifies that the algorithm can decelerate and change course of vessel properly in HO encounter according to the distribution of obstacles from 27s to 47s in the whole process, as shown in Figure 16(c-f). The minimum distance between vessel and the detected obstacles (including another vessel) is 45.7m, and the computation time is less 0.2s, see Figure 16(g) and 16(h).

b: CROSSING SITUATION

The second test case is crossing encounter with the TV approaching from the port of OV, and relative, OV approaches from the TV's starboard, meanwhile, both the OV and TV have the same initial speeds. The crossing encounter can

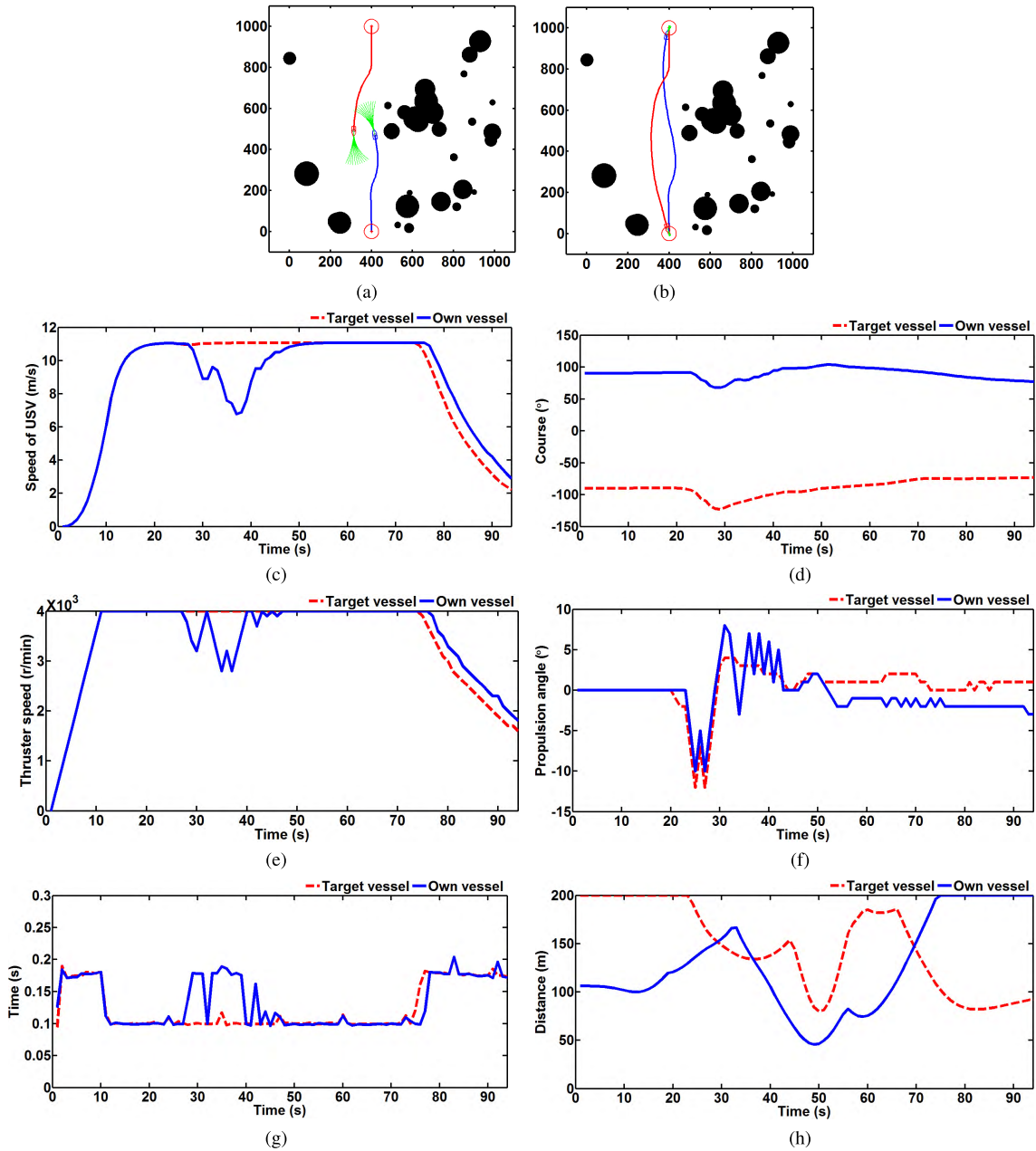


FIGURE 16. Motion simulation diagram and evaluation results of both vessels in Head-on situation. (a) The motion diagram with time 50s; (b) Time 94s; (c) Speed of vessel; (d) Course of vessel; (e) Thruster speed; (f) Command propulsion angle; (g) Computation time; (h) Distance between obstacles and vessel.

test whether CAS obeys COLREGs Rule 15. The motion diagram of the case is shown in Figure 17. According to Rule 15, the roles of the OV and TV are reversed from the perspective of the two vessels, in such case the OV is in LCS encounter, and not required to have the collision avoidance operation, whereas the TV is in RCS encounter, and needs to alter its course, crossing the OV at the stern from 18s to 29s. In the process of evading, the speed of both vessels changes little, their minimum distance is also large enough, and computation time less than 0.2s.

c: OVERTAKING SITUATION

The third test scenario is an OT scenario with the OV approaching the TV from the stern, and the maximum thruster speed of TV is limited to 2000r/min, which makes the speed of the OV greater than that of the TV throughout the simulation to overtake TV. The test is to assess whether CAS is complying with COLREGs Rule 13. The motion diagram of the test is shown in Figure 18. Because OV is in OT situation, OV needs to either port or starboard and overtake TV. In the test, there are not only TV but also static obstacles in the environment, so OV runs to port side of TV to avoid

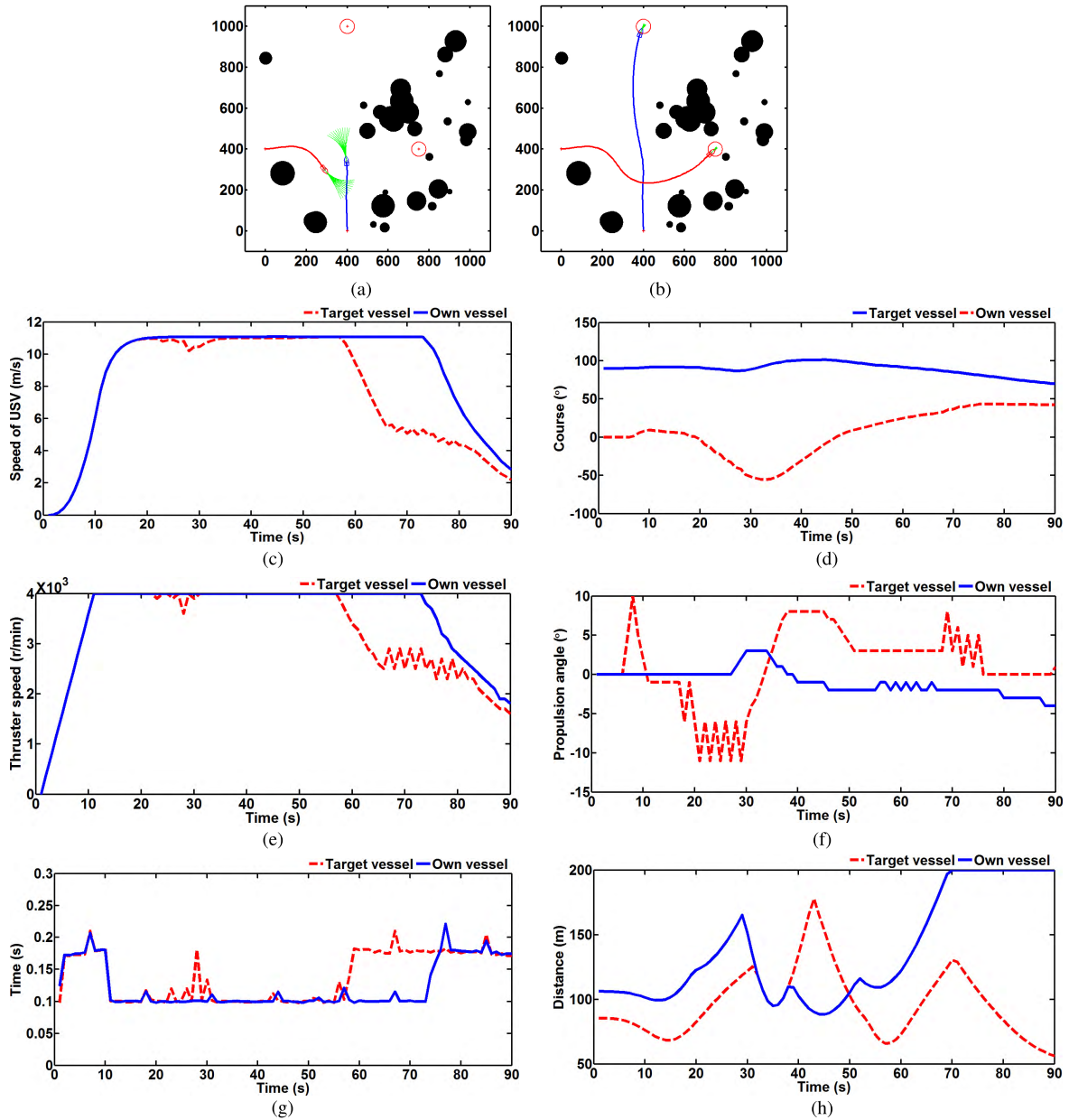


FIGURE 17. Motion simulation diagram and evaluation results of both vessels in Crossing situation. (a) The motion diagram with time 35s; (b) Time 90s; (c) Speed of vessel; (d) Course of vessel; (e) Thruster speed; (f) Command propulsion angle; (g) Computation time; (h) Distance between obstacles and vessel.

complicated environment, see Figure 18(a), 18(b). From Figure 18(g), 18(h), the distance and computation time meet the requirements of the system.

B. VERIFICATION IN REALISTIC SEA ENVIRONMENT

1) ACTUAL SEA ENVIRONMENT MODEL

The improved GoodWin ship domain model by Davis expands the USV into a circle with the radius R_{USV} of the half ship length [49]. According to (25), the radius R_{Obst} of the obstacle is further expanded to RR_{UO} .

$$RR_{UO} = R_{USV} + R_{Obst} \quad (25)$$

In this way, USV can be regarded as a particle, as shown in Figure 19. Therefore, the collision avoidance problem of

USV is converted to the expanded obstacle avoidance of the particle.

In addition, the height information in the environment is removed, considering only the two-dimensional (2D) plane environment. Therefore, the motion of the USV can be regarded as the particle motion in the plane environment.

The outer sea area of the harbor basin at Dalian Maritime University is selected as the marine environment modeling area. The marine environment in the electronic chart is shown in Figure 20.

There are islands and coastlines in the electronic chart. It is very necessary to deal with the coastline. Determine whether there is convex areas in the coastline, these areas are considered as an island. After excluding the convex region,

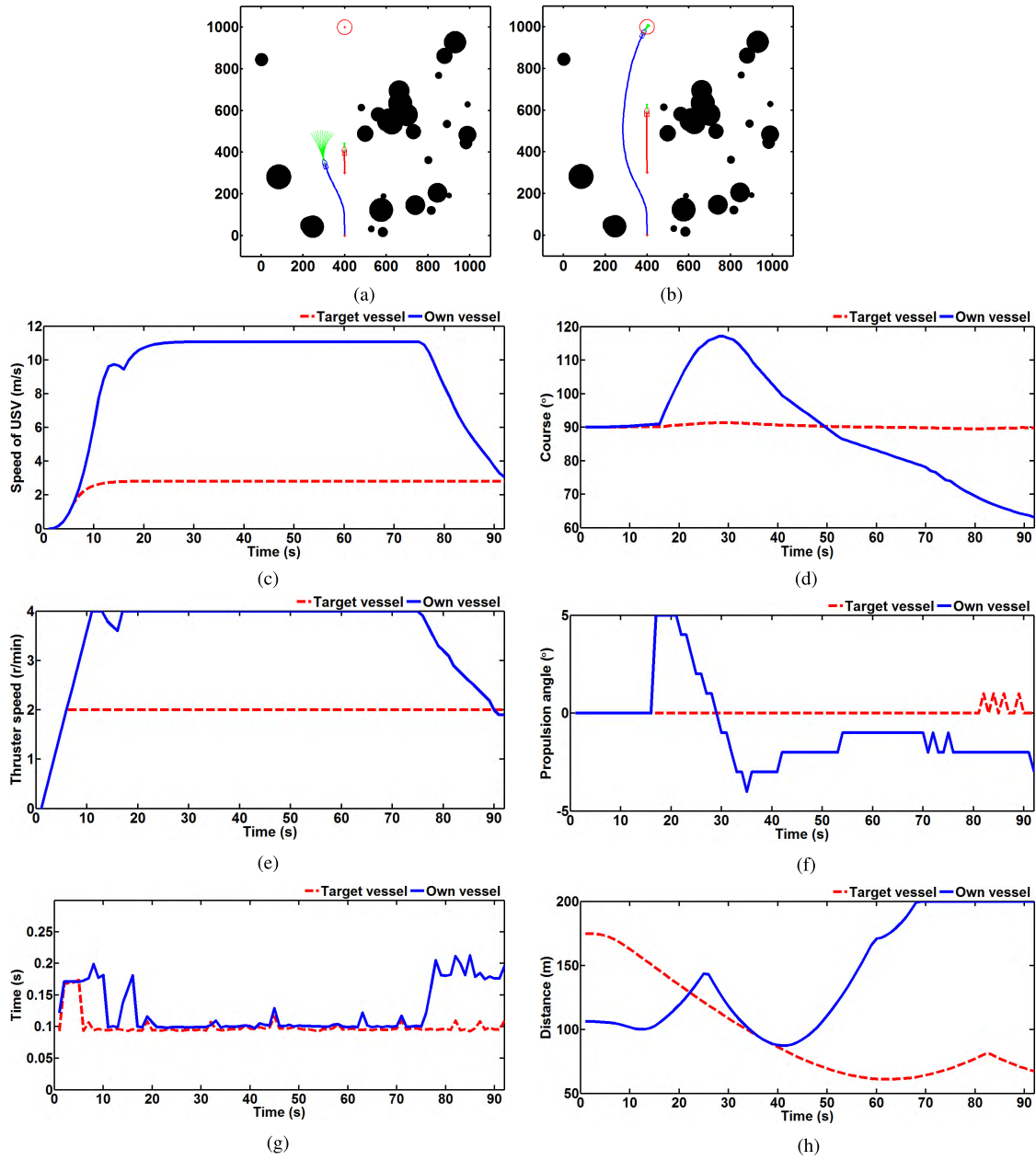


FIGURE 18. Motion simulation diagram and evaluation results of both vessels in Overtaking situation. (a) The motion diagram with time 37s; (b) Time 92s; (c) Speed of vessel; (d) Course of vessel; (e) Thruster speed; (f) Command propulsion angle; (g) Computation time; (h) Distance between obstacles and vessel.

the coastline is fitted as a line segment, and the farthest point of the coastline is calculated. The circumcircle of the farthest point and two ends of the fitted line segment is the approximate circle of the coastline, as shown in Figure 21.

These islands can be approximated as circles, calculating the center point (r_x, r_y) and radius r_0 of which is shown in (26).

$$\begin{cases} r_x = r_0 + x_{\min} \\ r_y = r_0 + y_{\min} \end{cases} \quad r_0 = \sqrt{[(x_{\max} - x_{\min})/2]^2 + [(y_{\max} - y_{\min})/2]^2} \quad (26)$$

where x_{\max}, x_{\min} and y_{\max}, y_{\min} are the maximum and minimum values of the islands on the x and y axes of the image coordinate system, respectively.

The simulated marine environment is shown in Figure 22.

Now, the environment model is completed, which provides the foundation for the CAS in real environment.

2) KINETIC EQUATION OF USV WITH MODEL UNCERTAINTIES AND EXTERNAL DISTURBANCES

According to [29] and [50], in order to verify the robustness of the CAS, the model uncertainties and external disturbances

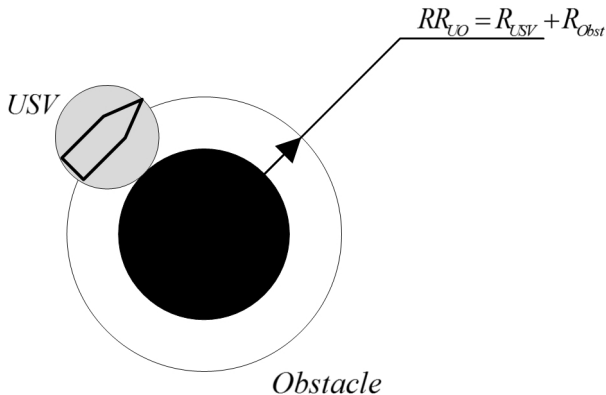


FIGURE 19. The expanded obstacle.



FIGURE 20. The marine environment in the electronic chart.

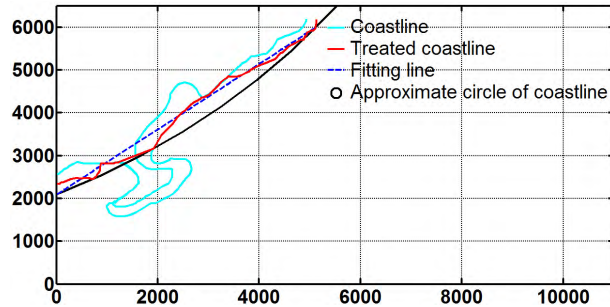


FIGURE 21. The coastline model after treatment.

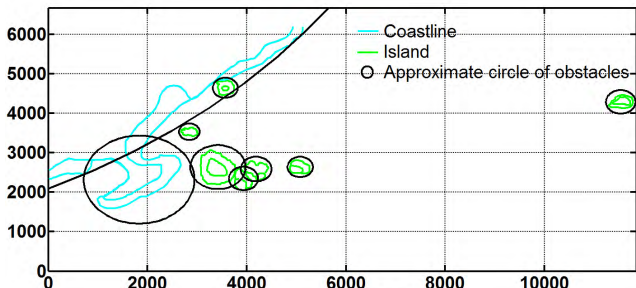


FIGURE 22. The expanded obstacle.

are added to the kinetic equation (6) of USV, which can be rewritten as

$$\begin{cases} \dot{u} = f_u + \frac{1}{m_{11}}(\tau_u + b_u - \Delta_u) \\ \dot{v} = f_v + \frac{1}{m_{22}}(\tau_v + b_v - \Delta_v) \\ \dot{r} = f_r + \frac{1}{m_{33}}(\tau_r + b_r - \Delta_r) \end{cases} \quad (27)$$

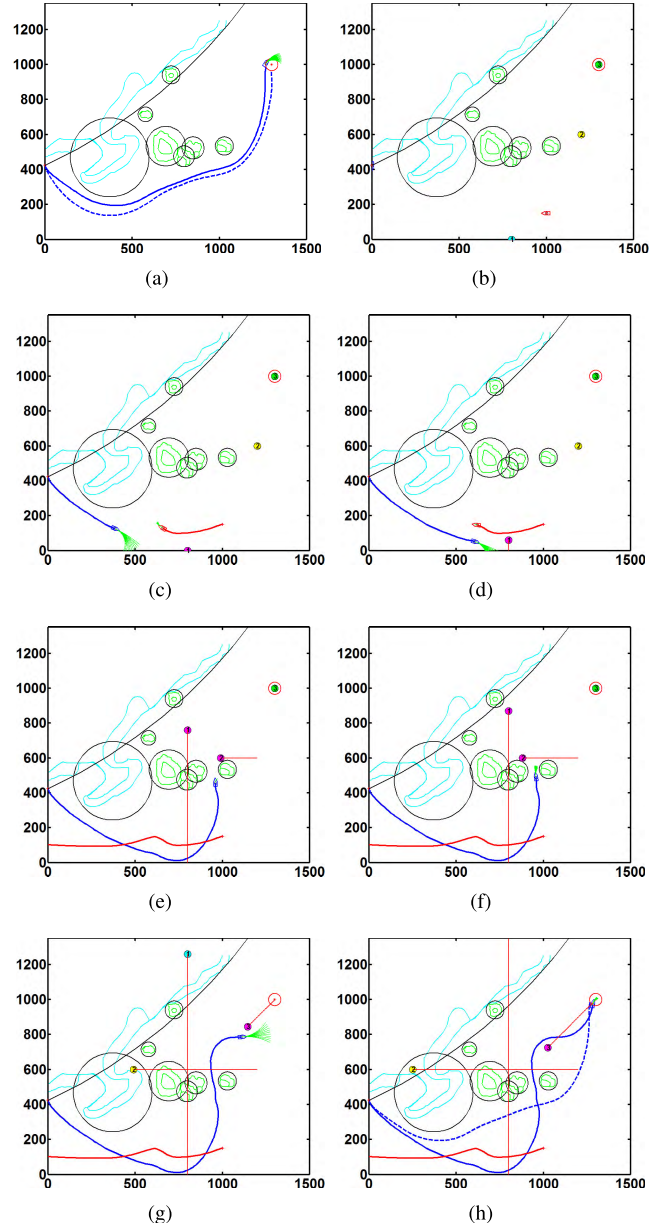


FIGURE 23. The motion sequence diagram of USV in static and dynamic realistic sea environment. (a) The final results in static environment; (b) The motion sequence diagram with time 1s in dynamic environment. (c) Time 43s. (d) Time 60s. (e) Time 130s. (f) Time 141s. (g) Time 180s. (h) Time 204s.

with $f_u = \frac{m_{22}}{m_{11}}vr - \frac{d_{11}}{m_{11}}u$, $f_v = -\frac{m_{11}}{m_{22}}ur - \frac{d_{22}}{m_{22}}v$, $f_r = \frac{m_{11}-m_{22}}{m_{33}}uv - \frac{d_{33}}{m_{33}}r$, and the external disturbances are assumed to be $b_u = 800[1 + 0.5 \sin(0.2t) + 0.3 \cos(0.5t)]$, $b_v = 800[1 + 0.5 \sin(0.2t) + 0.3 \cos(0.4t)]$, $b_r = 800[1 + 0.2 \sin(0.1t) + 0.2 \cos(0.2t)]$. Meanwhile, model uncertainties in each direction are $\Delta_u = 0.2f_u$, $\Delta_v = 0.2f_v$, $\Delta_r = 0.2f_r$.

3) SIMULATION VERIFICATION

Due to the open water is not suitable to verify the effectiveness of the algorithm, in order to make the environment more complex, we reduced the map by 5 times. In Figure 23, the static obstacles include islands and coastlines, which

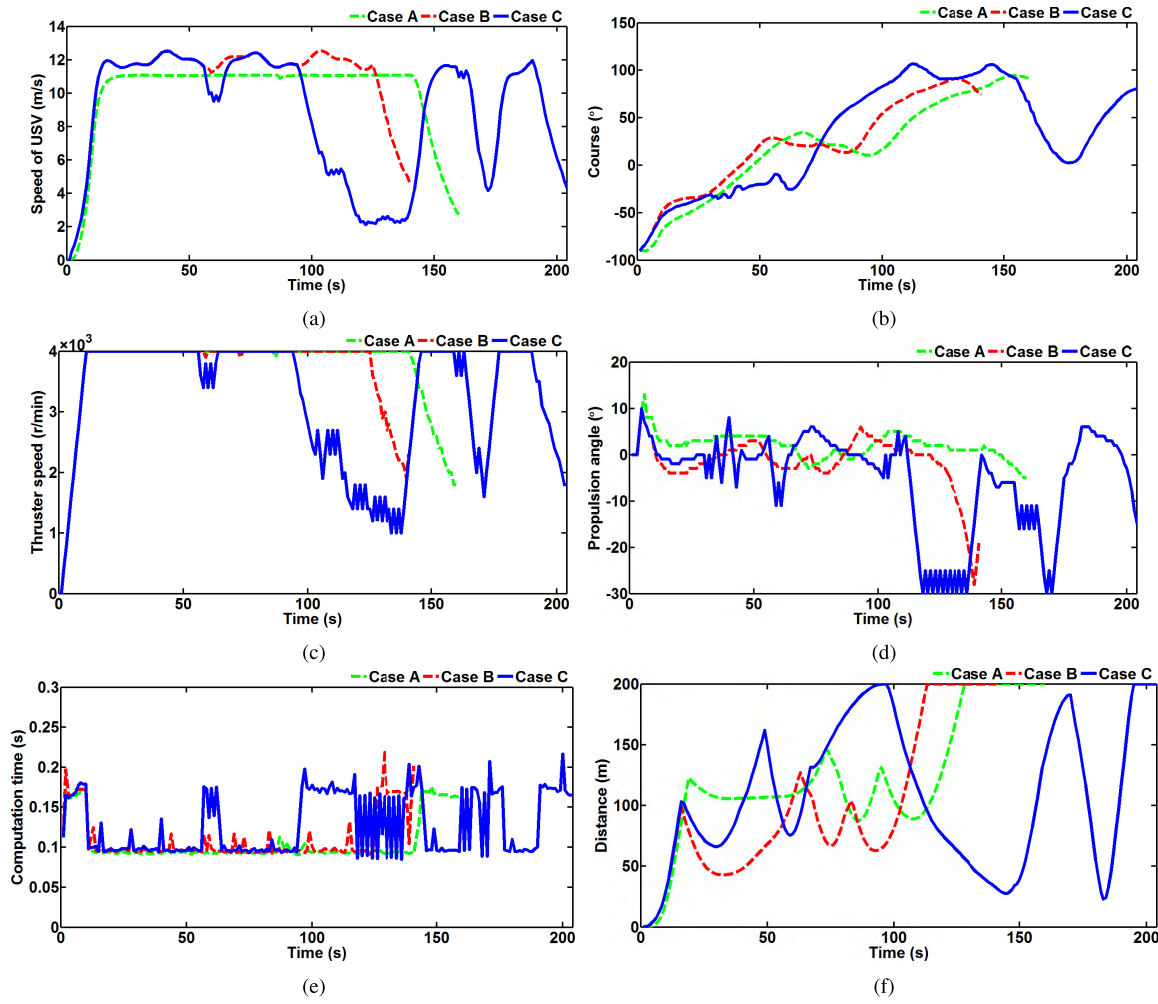


FIGURE 24. Evaluation results. (a) Speed of USV; (b) Course of USV; (c) Thruster speed; (d) Command propulsion angle; (e) Computation time; (f) Distance between obstacles and USV.

expand as circular obstacles required by the algorithm. Under the same system parameters condition, USV sails in the static environment, and Figure 23(a) shows the final results in the case of no-disturbances (blue solid curve) and disturbances (blue dashed curve). The trajectory of USV is shifted upward with disturbances, but USV can still safely avoid all obstacles to the end.

Now, three DOs and a TV are added into the environment traveling, where the speeds of DO1 and DO2 are 10m/s, DO3 is 7m/s. And TV and OV with model uncertainties and external disturbances have the same algorithmic parameters. The movement sequences are represented in Figure 23(b-h). In addition, the algorithm is verified in different obstacles and situations. Figure 23(b), 23(c) plot that the OV moving from the initial course to meet the TV and formed the Head-on situation, both vessels sail to each other's port side by COLREGs. After getting away from the TV, two RCS situations are made up of USV and DO1, DO2 in Figure 23(c-f), and Figure 23(d) displays the OV evasion process to alter course, crossing the DO1 at the stern. Especially in the evasion process for DO2, OV begins to enter the narrow waters. If keeps the current speed and alters course according to the rules, OV may

eventually collide with the static obstacles, so in this case, the CAS takes the action of slackening OV's speed to wait for the safe passing of the DO2 in Figure 23(e) and 23(f), which accord with Rule 8, paragraph e from COLREGs. When successfully avoids the DO1 and DO2, the OV approaches the DO3 head-on. As can be seen from Figure 23(g), although DO3 maintained its course in the process, OV still completed the task of head-on. Figure 23(h) shows the both the final trajectories of OV in static and dynamic environments.

The results of OV output and input with three cases, including case A (static environment without disturbances), case B (static environment with disturbances) and case C (dynamic environments with disturbances), are shown in Figure 24(a-d) and Table 4. In Table 4, since the starting point of the test is on the coastline, the initial section from 1s to 16s should be excluded during the calculation process of distance. In Figure 24(a), 24(c), with model uncertainties and external disturbances, the speed curve of USV is oscillation and its maximum value is increased compared with that in case A, and the course is also affected by the same factors in Figure 24(b). From Figure 24(d), due to the stability evaluation of algorithm, the average propulsion angle is close to 0°,

TABLE 4. Results of evaluation index comprised of two realistic environment.

Case	Index	Speed of USV(m/s)	Thruster speed(r/min)	Propulsion angle(°)	Computation time(s)	Distance(m)
A	maximum	11.0	4000	13.0	0.18	200.0
	minimum	0.0	0	-5.0	0.09	87.5
	average	9.9	3711	1.9	0.11	133.0
B	maximum	12.5	4000	10.0	0.22	200.0
	minimum	0.0	0	-28.0	0.09	43.0
	average	10.7	3694	-1.5	0.11	108.2
C	maximum	12.5	4000	10.0	0.22	200.0
	minimum	0.0	0	-30.0	0.08	23.0
	average	8.8	3214	-5.1	0.13	113.9

indicating that the propulsion angle rarely reaches the large propulsion angle or hard over angle. In the two cases of B and C, the minimum propulsion angle reaches or approaches the hard-a-starboard. In case B, the OV is affected by disturbances, and there is a certain deviation when approaching the end point, but due to the limitation of vessel maneuverability, it can only reach the end point by increasing the propulsion angle as much as possible. The hard-a-starboard in case C is in compliance with COLREGs. The first hard-a-starboard occurs in the narrow waters with RCS situation. And the second is affected by the disturbances with HO situation, so the OV needs to alter its course to starboard as far as possible to overcome the disturbances and obey the rules. Figure 24(e) displays the computing time is less than 0.22s. The distance is recorded in Figure 24(f). The average distance of case B is less than case A, which is due to disturbances. In case C, the minimum distances of four collision avoidance situations are respectively 75.4m, 131.2m, 107.2m and 23.0m, which means that the navigation of OV is safe with model uncertainties and external disturbances.

VII. CONCLUSIONS

In this paper, the CAS with COLREGs compliance has been proposed for the podded propulsion USV. Through the modeling and identification of the podded propulsion USV, and according to the COLREGs rules for the analysis of the five encounter situations, a CAS based on FCS-MPC method is designed. In the simulations, the USV makes decisions based on the state of the dynamic obstacles in encounter situations, and considers the course and speed changes according to the encounter situations. And the simulation results show that the proposed CAS is a practical and effective candidate for an autonomous USV.

Next, in order to enable the system to be used on real ship experiment, the CAS should be applied in a more realistic environment model instead of the ideal shape model. And considering that the sea environment is complicated and changeable, it is very necessary to further estimate the model uncertainties and external disturbances in a prediction horizon to improve the control accuracy of the CAS.

REFERENCES

- S. Campbell, W. Naeem, and G. W. Irwin, "A review on improving the autonomy of unmanned surface vehicles through intelligent collision avoidance manoeuvres," *Annu. Rev. Control*, vol. 36, no. 2, pp. 267–283, 2012.
- Z. Liu, Y. Zhang, X. Yu, and C. Yuan, "Unmanned surface vehicles: An overview of developments and challenges," *Annu. Rev. Control*, vol. 41, pp. 71–93, Jan. 2016.
- J.-Y. Zhuang, L. Zhang, S.-Q. Zhao, J. Cao, B. Wang, and H.-B. Sun, "Radar-based collision avoidance for unmanned surface vehicles," *China Ocean Eng.*, vol. 30, no. 6, pp. 867–883, 2016.
- P. Tang, R. Zhang, D. Liu, L. Huang, G. Liu, and T. Deng, "Local reactive obstacle avoidance approach for high-speed unmanned surface vehicle," *Ocean Eng.*, vol. 106, pp. 128–140, Sep. 2015.
- J. Woo and N. Kim, "Vision-based target motion analysis and collision avoidance of unmanned surface vehicles," *Proc. Inst. Mech. Eng. M, J. Eng. Maritime Environ.*, vol. 230, no. 4, pp. 566–578, 2016.
- G. Zhang, Y. Deng, and W. Zhang, "Robust neural path-following control for underactuated ships with the DVS obstacles avoidance guidance," *Ocean Eng.*, vol. 143, pp. 198–208, Oct. 2017.
- COLREGs—Convention on the International Regulations for Preventing Collisions at Sea*, Int. Maritime Org., London, U.K., 1972.
- W. Naeem, G. W. Irwin, and A. Yang, "COLREGs-based collision avoidance strategies for unmanned surface vehicles," *Mechatronics*, vol. 22, no. 6SI, pp. 669–678, 2012.
- T. Statheros, G. Howells, and K. M. Maier, "Autonomous ship collision avoidance navigation concepts, technologies and techniques," *J. Navigat.*, vol. 61, no. 1, pp. 129–142, 2008.
- Y.-L. Lee, S.-G. Kim, and Y.-G. Kim, "Fuzzy relational product for collision avoidance of autonomous ships," *Intell. Automat. Soft Comput.*, vol. 21, no. 1, pp. 21–38, 2015.
- Y. Kuwata, M. T. Wolf, D. Zarzhitsky, and T. L. Huntsberger, "Safe maritime autonomous navigation with COLREGS, using velocity obstacles," *IEEE J. Ocean. Eng.*, vol. 39, no. 1, pp. 110–119, Jan. 2014.
- I. R. Bertaska et al., "Experimental evaluation of automatically-generated behaviors for USV operations," *Ocean Eng.*, vol. 106, pp. 496–514, Sep. 2015.
- Y. Zhao, W. Li, and P. Shi, "A real-time collision avoidance learning system for unmanned surface vessels," *Neurocomputing*, vol. 182, pp. 255–266, Mar. 2016.
- J. Zhang, D. Zhang, X. Yan, S. Haugen, and C. G. Soares, "A distributed anti-collision decision support formulation in multi-ship encounter situations under COLREGS," *Ocean Eng.*, vol. 105, pp. 336–348, Sep. 2015.
- S. Campbell, M. Abu-Tair, and W. Naeem, "An automatic COLREGS-compliant obstacle avoidance system for an unmanned surface vehicle," *Proc. Inst. Mech. Eng. M, J. Eng. Maritime Environ.*, vol. 228, no. 2, pp. 108–121, 2014.
- Q. Xu, C. Zhang, and N. Wang, "Multiobjective optimization based vessel collision avoidance strategy optimization," *Math. Problems Eng.*, vol. 2014, Feb. 2014, Art. no. 914689.
- T. A. Johansen, T. Perez, and A. Cristofaro, "Ship collision avoidance and COLREGs compliance using simulation-based control behavior selection with predictive hazard assessment," *IEEE Trans. Intell. Transp. Syst.*, vol. 17, no. 12, pp. 3407–3422, Dec. 2016.
- W. H. Li, Y. Q. Sun, H. Chen, and G. Wang, "Model predictive controller design for ship dynamic positioning system based on state-space equations," *J. Mar. Sci. Technol.*, vol. 22, no. 3, pp. 426–431, Sep. 2017.
- Z. Li and J. Sun, "Disturbance compensating model predictive control with application to ship heading control," *IEEE Trans. Control Syst. Technol.*, vol. 20, no. 1, pp. 257–265, Jan. 2012.
- S.-R. Oh and J. Sun, "Path following of underactuated marine surface vessels using line-of-sight based model predictive control," *Ocean Eng.*, vol. 37, nos. 2–3, pp. 289–295, Feb. 2010.
- Z. Yan and J. Wang, "Model predictive control for tracking of underactuated vessels based on recurrent neural networks," *IEEE J. Ocean. Eng.*, vol. 37, no. 4, pp. 717–726, Oct. 2012.
- J. Wu, H. Peng, K. Ohtsu, G. Kitagawa, and T. Itoh, "Ship's tracking control based on nonlinear time series model," *Appl. Ocean Res.*, vol. 36, pp. 1–11, Aug. 2012.

- [23] C. Xia, T. Liu, T. Shi, and Z. Song, "A simplified finite-control-set model-predictive control for power converters," *IEEE Trans. Ind. Informat.*, vol. 10, no. 2, pp. 991–1002, May 2014.
- [24] D. Song, J. Yang, M. Dong, and Y. H. Joo, "Model predictive control with finite control set for variable-speed wind turbines," *Energy*, vol. 126, pp. 564–572, May 2017.
- [25] M. A. Abkowitz, "Lectures on ship hydrodynamics: Steering and manoeuvrability," Hydro' Aerodyn. Lab., Lyngby, Denmark, Tech. Rep. Hy-5, 1964.
- [26] N. H. Norrbin, "Theory and observations on the use of a mathematical model for ship manoeuvring in deep and confined waters," in *Proc. 8th Symp. Nav. Hydrodyn.*, Pasadena, CA, USA, 1970, pp. 807–904.
- [27] A. Ogawa, T. Koyama, and K. Kijima, "MMG report-I, on the mathematical model of ship manoeuvring," *Bull. Soc. Nav. Archit. Jpn.*, vol. 575, pp. 22–28, 1977. [Online]. Available: <https://scholar.google.com/scholar?q=Ogawa%2C%20A.%2C%20Koyama%2C%20T.%2C%20Kijima%2C%20K.%3A%20MMG%20report-I%2C%20on%20the%20mathematical%20model%20of%20ship%20manoeuvring%20%28in%20Japanese%29.%20Bull%20Soc.%20Naval%20Archit.%20Jpn.%20575%2C%2022%2E%80%9328%20%281977%29> and [https://link.springer.com/article/10.1016/S1001-6058\(16\)60630-3](https://link.springer.com/article/10.1016/S1001-6058(16)60630-3)
- [28] T. I. Fossen, *Nonlinear Modelling and Control of Underwater Vehicles*. Trondheim, Norway: Fakultet for informasjonsteknologi, matematikk og elektroteknikk, 1991.
- [29] T. I. Fossen, *Handbook of Marine Craft Hydrodynamics and Motion Control*. Hoboken, NJ, USA: Wiley, 2011.
- [30] W. Gierusz, "Simulation model of the LNG carrier with podded propulsion, part II: Full model and experimental results," *Ocean Eng.*, vol. 123, pp. 28–44, Sep. 2016.
- [31] M. Reichel, "Prediction of manoeuvring abilities of 10000 DWT pod-driven coastal tanker," *Ocean Eng.*, vol. 136, pp. 201–208, May 2017.
- [32] D. Mu, G. Wang, Y. Fan, and Y. Zhao, "Modeling and identification of podded propulsion unmanned surface vehicle and its course control research," *Math. Problems Eng.*, vol. 2017, Apr. 2017, Art. no. 3209451.
- [33] X.-G. Wang, Z.-J. Zou, L. Yu, and W. Cai, "System identification modeling of ship manoeuvring motion in 4 degrees of freedom based on support vector machines," *China Ocean Eng.*, vol. 29, no. 4, pp. 519–534, 2015.
- [34] M. Cooper and L. McCue, "Design of a controller for autonomous vessel recovery utilizing the prediction of host vessel motions," *Nav. Eng. J.*, vol. 129, no. 1, pp. 117–131, 2017.
- [35] W. Luo, L. Moreira, and C. G. Soares, "Manoeuvring simulation of catamaran by using implicit models based on support vector machines," *Ocean Eng.*, vol. 82, pp. 150–159, May 2014.
- [36] C. Jian et al., "Parametric estimation of ship maneuvering motion with integral sample structure for identification," *Appl. Ocean Res.*, vol. 52, pp. 212–221, Aug. 2015.
- [37] M. Zhu, A. Hahn, Y.-Q. Wen, and A. Bolles, "Identification-based simplified model of large container ships using support vector machines and artificial bee colony algorithm," *Appl. Ocean Res.*, vol. 68, pp. 249–261, Oct. 2017.
- [38] W. Luo, C. G. Soares, and Z. Zou, "Parameter identification of ship maneuvering model based on support vector machines and particle swarm optimization," *J. Offshore Mech. Arctic Eng.*, vol. 138, no. 3, p. 031101, 2016.
- [39] G. Zhang, X. Zhang, and H. Pang, "Multi-innovation auto-constructed least squares identification for 4 DOF ship manoeuvring modelling with full-scale trial data," *ISA Trans.*, vol. 58, pp. 186–195, May 2015.
- [40] J. Yin, Z. Zou, and F. Xu, "Parametric identification of Abkowitz model for ship maneuvering motion by using partial least squares regression," *J. Offshore Mech. Arctic Eng.*, vol. 137, no. 3, p. 031301, 2015.
- [41] S. Baňka, M. Brasel, P. Dworak, and K. Jaroszewski, "A comparative and experimental study on gradient and genetic optimization algorithms for parameter identification of linear MIMO models of a drilling vessel," *Int. J. Appl. Math. Comput. Sci.*, vol. 25, no. 4, pp. 877–893, 2015.
- [42] S. Sutulo and C. G. Soares, "An algorithm for offline identification of ship manoeuvring mathematical models from free-running tests," *Ocean Eng.*, vol. 79, pp. 10–25, Mar. 2014.
- [43] L. P. Perera, P. Oliveira, and C. G. Soares, "System identification of vessel steering with unstructured uncertainties by persistent excitation maneuvers," *IEEE J. Ocean. Eng.*, vol. 41, no. 3, pp. 515–528, Jul. 2016.
- [44] W. Dong and Y. Guo, "Global time-varying stabilization of underactuated surface vessel," *IEEE Trans. Autom. Control*, vol. 50, no. 6, pp. 859–864, Jun. 2005.
- [45] T. I. Fossen, *Guidance and Control of Ocean Vehicles*. Hoboken, NJ, USA: Wiley, 1994.
- [46] X. Jia and Y. Yang, *The Mathematical Model of Ship Motion Mechanism Modeling and Identification Modeling*. Dalian, China: Dalian Maritime Univ. Press, 1999.
- [47] X. J. Sun, L. L. Shi, Y. S. Fan, and G. F. Wang, "Online parameter identification of USV motion model," *Navigat. China*, vol. 39, no. 1, pp. 39–43, 2016.
- [48] B. C. Shah et al., "Resolution-adaptive risk-aware trajectory planning for surface vehicles operating in congested civilian traffic," *Auton. Robots*, vol. 40, no. 7, pp. 1139–1163, 2016.
- [49] N. Wang, X. Meng, Q. Xu, and Z. Wang, "A unified analytical framework for ship domains," *J. Navigat.*, vol. 62, no. 4, pp. 643–655, 2009.
- [50] D. Mu, G. Wang, Y. Fan, B. Qiu, and X. Sun, "Adaptive trajectory tracking control for underactuated unmanned surface vehicle subject to unknown dynamics and time-varying disturbances," *Appl. Sci.*, vol. 8, no. 4, p. 547, Apr. 2018.



XIAOJIE SUN received the M.E. degree in control engineering from Dalian Maritime University, Dalian, China, in 2016, where he is currently pursuing the Ph.D. degree in control theory and control engineering. His research interests focus on the sea traffic management and unmanned surface vehicle system, such as modeling and collision avoidance.



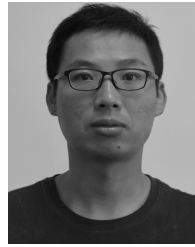
GUOFENG WANG received the B.E., M.E., and Ph.D. degrees from Dalian Maritime University, Dalian, China. He is currently a Professor with the School of Marine Electrical Engineering, Dalian Maritime University. He is engaged in the technical research of marine automation system and automation equipment, and has presided over and participated in a number of national and ministerial projects. His research interests include ship automation, advanced ship borne detection device, and advanced power transmission.



YUNSHENG FAN received the B.E., M.E., and Ph.D. degrees from Dalian Maritime University, Dalian, China, in 2004, 2007, and 2012, respectively. He is currently an Associate Professor with the School of Marine Electrical Engineering, Dalian Maritime University. His research interests are ship intelligent control and its application.



DONGDONG MU received the M.E. degree in control theory and engineering from Dalian Maritime University, Dalian, China, in 2015, where he is currently pursuing the Ph.D. degree in control theory and control engineering. His research interests include modeling and intelligent control of unmanned surface vehicle.



BINGBING QIU received the M.E. degree in control theory and engineering from Dalian Maritime University, Dalian, China, in 2017, where he is currently pursuing the Ph.D. degree in control theory and control engineering. His research interests include nonlinear control and intelligent control of unmanned surface vehicle.